Earthquake Geodynamics

Seismic Case Studies

Editor: E.L. Lekkas

WITPRESS

CHAPTER 9

Seismically-triggered landslide risk assessment

I. Parcharidis[1], Emm. Vassilakis[1], Ger. Cooksley[2] & Chr. Metaxas[3]
[1]*Faculty of Geology, University of Athens, Greece.*
[2]*NPA Group, UK.*
[3]*Earthquake Planning & Protection Organization, Athens, Greece.*

Abstract

Landslides can present a significant risk to people living in earthquake-prone areas. The use of geographical information systems (GIS) with relevant geophysical data and methods could be used to predict areas according to the risk of landslide occurrence. This study (part of the E.C. project SNAP) presents an application of a simplified Newmark method for modelling the seismically-triggered landslide risk in the broader area of Patras city (Achaia Prefecture) which is characterized of high seismic activity. The final risk map, which was produced using the Newmark method, appears to be highly correlated with landslides mapped on the field, showing a relative overlapping.

1 Introduction

Slopes failures during an earthquake may cause a great number of casualties and damage to structures and facilities. A landslide will occur when the stress acting on a slope exceeds the strength of the material forming the slope. This is expressed as the factor of safety (FoS). Usually the causes of a landslide can be divided into those that (i) increase the stress on a slope and (ii) decrease the strength of the materials that make up the slope. One of the mechanisms by which the factor of safety of a slope can be reduced is the triggering due to earthquakes, traffic, blasting etc. This study describes the development of an information system for seismically-triggered landslide risk assessment in the Achaia area (western Corinthian gulf).

A number of researchers worked on this topic, including the following recent studies. Ambraseys & Srbulov [1] studied the empirical predictive relations that allow an estimation of co-seismic sliding of slopes from the size of energy released by an earthquake in terms of its magnitude *(Ms)*, its distance from a site *(r)*, and from the critical acceleration ratio $q=Kc/Kmv$. The authors used the sliding block method to calculate permanent displacements. The same authors [2] described a method for estimation of post-seismic sliding for translational slides.

Tibaldi *et al.* [3] examined landslides triggered by earthquakes and their relations with faults and slope geometry. Landslide distribution shows a correlation with respect to the dip-direction of the faults and the orientation of mountain slopes. Hirotaka *et al.* [4] examined the landslides induced by the Kobe earthquake in Rokko Mountain. In this case the area of the landslide limit was low in relation to historical worldwide earthquakes of this magnitude, probably as a result of the shallow source of the main shock. The reasons for the low number of landslides were the fairly good bedrock, the dry antecedent condition in winter and the existence of forest cover.

Srbulov [5] estimated sliding of slopes during earthquakes using Monte Carlo simulation based on a semi-empirical attenuation relation and using adopted probability density functions of the parameters in the relation. According to the authors Monte Carlo simulation should be considered for estimations only.

Mankelow & Murphy [6] attempted a landslide hazard zoning using GIS in a probabilistic approach in the assessment of earthquake-triggered landslide hazard.

Luzi & Pergalani [7], basing their studies on the case of the Umbria-Marche earthquake (26 September 1997), tested the prediction accuracy of empirical equations to calculate landslide displacement. Accelerometric records from the permanent and mobile seismic network of the Seismic Survey of Italy were processed and interpolated in order to obtain strong motion parameters at each terrain unit and possible displacements. The results were compared to verify the prediction, given the real landslide occurrences. The method based on Destructiveness Potential was, according to the authors, the most accurate.

Murphy *et al.* [8] considered three cases of landslides triggered by earthquakes and studied the natural variability of the slope-forming materials and the uncertainties surrounding input ground motions. The results of the analyses show a large scatter into calculated factors of safety for earthquake conditions. The models used in the calculation of seismic slope stability yield acceptable results.

This study describes an assessment of seismically-triggered landslides in the area of Achaia (western Corinthian gulf) using GIS based on the Newmark method [9].

2 Geological setting of the area

The dominant orientation of the mountains of the wider study area is NW–SE. These mountains were formed during the Alpine orogeny and they are a recurrence of the mountain ranges of central Greece and Epirus. The main hydrographic network in the Achaia area consists of inflow basins for the rivers Vouraikos, Selinous, Glafkos, Peiros and Foinikas. These rivers flow generally from south to north and are strongly affected by the morphology as this was formed due to high neotectonic activity. Significant quantities of deposits, arising mainly from erosion of Pleio-Pleiostocene formations as well as of later formations, are transported to the coast of the Corinthian Gulf.

The geology of the Achaia consists mainly of alpine sediments of the geotectonic units (from east to west): Pindos, Gavrovo and Ionian. These units are partially covered by Neogene to Quaternary deposits. After studying the geological maps in 1:50 000, the following can be noted:

a) Ionian unit: There is a small appearance in the Western part of the Achaia, due to concealment by Neogene and Quaternary deposits. In particular the internal area of the Ionian unit appears at Manolada where limestone formations from the Upper Jurassic to the Lower Eocene arise, while on these Eocene flysch is deposited.

b) Gavrovo unit: This appears in the western and eastern part of the Achaia. This unit consists of limestone formations, gypsum, dolomitic limestone and schists.

c) Pindos unit: Appearing in the centre of Achaia and consisting of the following alternations: Volcanic tuffs, Triassic – L. Jurassic limestone, L. Cretaceous cherts and radiolarites, Up. Cretaceous limestone and Eocene flysch.

These three units are covered in a large part of the Achaia Perfecture by Pleiocene and other Quaternary formations. These formations can be defined as:

a) Pleio-Pleistocene deposits which consist of marls, clays, sands and conglomerates.

b) Dilouvial deposits which consist of mixed phases of conglomerates with marls and pieces of fragments of erosion, as well as of bigger and smaller pieces of conglomerates and loose or connected material.

c) Holocene deposits which are alluvial deposits and recent silt. These are completed by lagoonal or lake deposits as well as coastal sand formations.

The seismological data which are available for the Achaia area are divided into two periods. The first period consists of earthquakes up to 1889, while the second comprises those from 1900 up to today.

Figure 1 shows the distribution of earthquake epicenters with a magnitude greater than 4.5 Ms for the period 1900–today and within a radius of 100 km

around the city of Patras. As shown in Figure 1, there is a concentration of seismicity along the line Lake Trichonis - Gulf of Corinth and there is less seismicity in the immediate vicinity of the city of Patras. The Gulf of Patras corresponds to a seismic gap where according to Hatzfeld *et al.* [10] there is no observed seismicity at all, even for small magnitude events (microearthquakes). The focal depths of the earthquakes with epicenters around the Gulf of Patras are in the range 5–20 km.
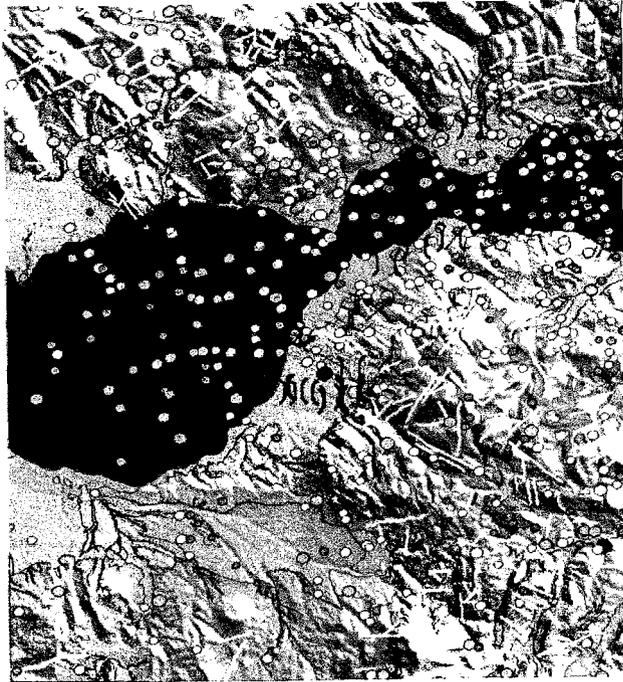

Figure 1: Distribution of earthquake epicenters with magnitude greater than 4.5 Ms for the period 1900–today.

The wider area of Patras is the westernmost part of an asymmetric graben system striking WNW–ESE, which characterizes the tectonic regime of Central Greece. This system has an age of 3 my and consists of the Saronic Gulf - Gulf of Corinth - Gulf of Patras and Trichonis lake. These grabens were formed under an extensional regime which has been dominant until today in the central Greece area, with strike direction N–S and with a rate of 1.5 cm/y.

Micro-earthquake and tectonic studies in the area of the Achaia and western Greece, showed that the Saronic-Corinth-Trichonis system links to Patras through an asymmetric graben (Rio-Antrrio) which shows complicated rupture characteristics, that is, extensional (normal) and dextral horizontal (strike-slip)

(Vassilakis [11]). Armijo *et al.* [12] suggested that this small graben is the link between Patras and the gulf of Corinth which, according to the spatial distribution of micro-earthquakes in the narrow area from the western Corinth Gulf up to Trichonis to the East, links to Trichonis lake.

An important observation shows that the gulf of Patras is a shallow graben where there is no seismicity of any range of magnitude. On the other hand, the eastern side of the Patras gulf and the area south of Patras city where the link of the Rio-Antirrio system, historical earthquakes of maximum magnitude 6.7 Ms, as well as seismic records (recorded events) with magnitude 5.5 Ms, have been observed (Tselentis & Makropoulos [13]).

It is also important to note that high seismic activity with small magnitude events has been observed in the Rio-Antirrio area where the graben links to the Corinth-Trichonis system. A maximum magnitude of 6.7 Ms, has also been observed in the recorded incidents and in the historical catalogues.

In this study a database was created containing all the registered mapped neotectonic faults in the Achaia area, and the maximum expected earthquake magnitude was estimated for each of the registered faults. For the wider area of Patras, the maximum expected earthquake magnitude is not more than 5.9 Ms, while it is important to note that there was a historical event of 6.7 Ms in the same area.

3 Data collection and database construction

Seismically triggered landslides can represent a significant risk to people living in earthquake-prone regions. The use of GIS with relevant geophysical data and methods can go some way to predicting and zoning areas according to the risk of landslide occurrence. Such maps can be used by the disaster-prevention community to guide disaster preparedness procedures as well as in making planning decisions to avoid new developments in those regions deemed to be at highest risk from landslides.

3.1 Analysis method

As part of an EC-funded study of the use of InSAR for seismic risk in Greece, the seismically-triggered landslide risk of an area around Patras was examined.

An implementation of the simplified Newmark method by Jibson *et al.* [14] was used to model seismically-triggered landslide risk. The landslide is modeled as a solid block sliding on an inclined plane. The block begins sliding when the forces exerted on it by the earthquake shaking exceed its critical acceleration threshold (a_c). The critical acceleration threshold of a potential landslide block is a function of the static factor of safety (Figure 2) and slope angle (Figure 3).

The acceleration time-history of an earthquake is normally used to calculate the displacement of the block. Accelerations above the critical threshold cause

the block to move while those below the threshold have no effect upon it. The critical acceleration of a block (in terms of the Earth's gravity g) is given by:

$$a_c = (FS - 1)g \sin \alpha \tag{1}$$

where *FS* is the static factor of safety and α is the slope angle. The slope angle data were generated from a three-arc second resolution DEM of the region.
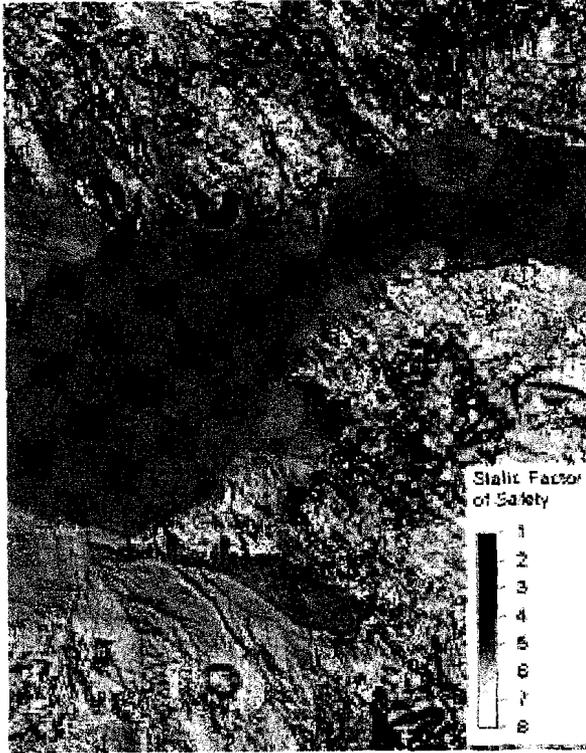

Figure 2: Static factor of safety.

3.2 Static factor of safety

The static factor of safety (FS) is an expression of the balance between resisting and driving forces acting upon the block (Jibson *et al.* [14]) and can be given by:

$$FS = \frac{c' + c'_r}{\gamma t \sin \alpha} + \frac{\tan \phi'}{\tan \alpha} - \frac{m \gamma_w \tan \phi'}{\gamma \tan \alpha} \tag{2}$$

cohesive + frictional – reduction of frictional
strength   strength   strength due to saturation

where c' is the cohesion, ϕ' is the friction angle, α is the slope angle, γ is the material unit weight γ_w is the unit weight of water, t is the thickness of the block, and m is the proportion of the slab that is water saturated. c'_r is an additional factor included to account for the added cohesion provided by tree roots as suggested by McCalpin [15]. The cohesion, friction angles and material weight were derived from a Geotechnical map (1:50 000, Patras) and applied to the geological units of a same-scale geological map digitized by E.P.P.O. The block thickness was set to 2.4 m following Jibson *et al.* [14]. A map of tree coverage (Figure 4) was derived from classifying Landsat ETM images; typical values for the added cohesion were as used by McCalpin [15].
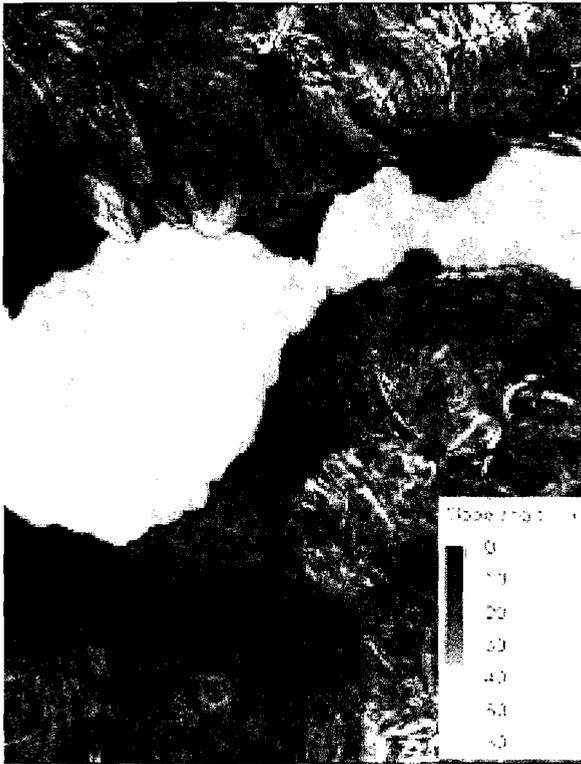

Figure 3: Slope map generated from DEM.

3.3 Newmark displacement calculation

The Newmark displacement calculation method used in this work was based on that presented by McCalpin [15] and utilized methods developed by Jibson [16] and Dobry *et al.* [17]. These methods use simple formulas developed from the regression analysis of earthquake time histories to provide a relationship

between predicted Newmark displacement (D_n), Arias Intensity (measure of ground motion) (I_a) and critical acceleration a_c:

$$\log D_n = 1.521 \log I_a - 1.993 \log a_c - 1.546 \qquad (3)$$

The data available for the Patras region lacked only earthquake strong motion records and groundwater depth data of sufficient density. This necessitated some modification of the above equations. Primarily, since sufficient groundwater data were not available, the proportion of the slab saturated was set to zero so that the third factor was removed from equation 2.
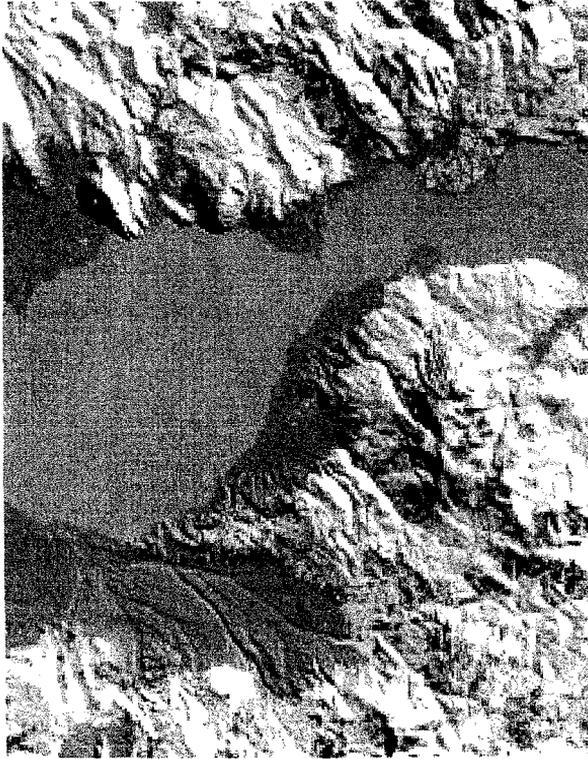

Figure 4: Tree coverage derived from classifying Landsat ETM data.

The second change that had to be made was to use an alternative source of earthquake ground intensity information to derive the Arias intensity. This method, proposed by McCalpin [15], utilized an equation presented by Wilson & Keefer [18] (cited in Jibson [15]) relating PGA with Arias Intensity (I_a):

$$I_a = 0.9(10^{0.432M-1.83})(PGA)^2 \qquad (4)$$

where M is earthquake magnitude.

The peak ground acceleration (PGA) data used (Figure 5) were published as part of the GSHAP (Global Seismic Hazard Assessment Programme) (Gruenthal *et al.* [19]), of which the Greek element was compiled by Makropoulos K. *et al.*, Athens University. The predicted Newmark displacements were calculated and used to generate a map of seismically triggered landslide risk (Figure 6).
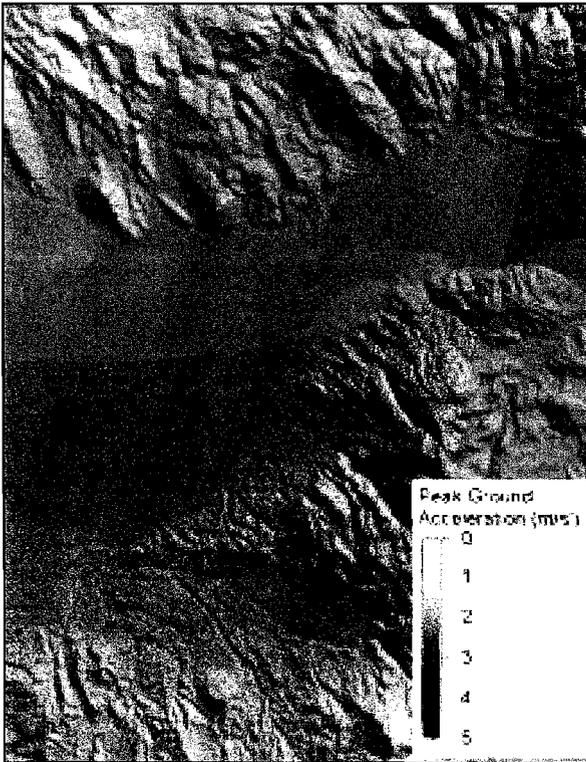

Figure 5: Seismic hazard map overlain on DEM showing the peak ground acceleration (m/s²) which there is a 10% likelihood of exceeding within 50 years (475 year return period).

4 Results and conclusions

Newmark analysis methods facilitated the production of a seismically triggered landslide risk map (Figure 6). This map could be used as a guide to areas that may need further investigation and could ultimately be used for zoning

earthquake risk areas. It would, however, be worthwhile to conduct further Newmark displacement analyses of the region, particularly by using groundwater depth information and actual earthquake strong motion records for the derivation of the Arias Intensity.
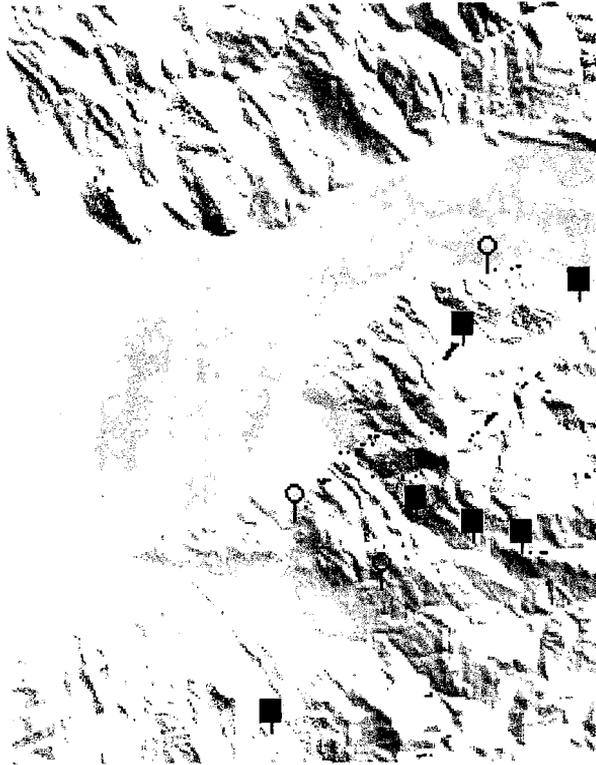

Figure 6: Areas of high seismically-triggered for landslide risk (black pixels). The circles represent landslides triggered by recent earthquakes, while the square symbols represent landslides due to other causes.

References

[1]   Ambraseys, N. & Srbulov, M., Attenuation of earthquake induced displacements. *J. Earthq. & Struct. Dyn.*, **23**, pp. 467–487, 1994.
[2]   Ambraseys, N. & Srbulov, M., Earthquake induced displacements of slopes. *Soil Dyn. and Earthq. Engineering*, **14**, pp. 59–71, 1995.

[3] Tibaldi A., Ferrari, L. & Pasquare G., Landslides triggered by earthquakes and their relations with faults and mountain slope geometry: an example from Ecuador. *Geomorphology*, **11(3)**, pp. 215–226, 1995.

[4] Hirotaka, O., Hikaru, K., Toshiaki, S. & Kazutoki A., Landslides triggered by the 1995 Hyogo-Ken Nanbu earthquake in the Rokko mountains. *Landslides,* Senneset, Balkema, Rotterdam, 1996.

[5] Srbulov, M., Estimation of co-seismic sliding of slopes. *Landslides,* Senneset, Balkema, Rotterdam. 1996.

[6] Mankelow, M. & Murphy, W., Using GIS in the probabilistic assessment of earthquake triggered landslide hazard. *J. Earth Engin.*, **2(4)**, pp. 593–623, 1998.

[7] Luzi, L. & Pergalani, F., A correlation between slope failures and accelerometric parameters: the 26 September 1997 earthquake (Umbria-Marche, Italy). *Soil Dynamics and Earthquake Engineering*, **20**, pp. 301–313, 2000.

[8] Murphy, W., Petley D.N., Bommer, J. & Mankelow J.M., Uncertainty in ground motion estimates for the evaluation of slope stability during earthquakes. *Quaternarly Journal of Engineering Geology and Hydrology.* **35(1)**, pp. 71–78, 2002.

[9] Newmark, M., Effects of earthquakes on dams and embankments. *Geotechnique*, **15(2)**, pp. 139–160, 1965.

[10] Hatzfeld, D., Karakostas, V., Ziazia, M., Kassaras, J., Papadimitriou, E., Makropoulos, K., Voulgaris, N. & Papaioannou, C., Microseismicity and faulting geometry in the Gulf of Corinth (Greece). *Geophysical Journal International,* **141(2)**, pp. 438–456, 2000.

[11] Vassilakis, Emm., *Neotectonic regime of the Central Aetolia & Akarnania*, MSc Thesis, National & Capodestrian University of Athens, 1998.

[12] Armijo, R., Meyer, B., King, G. & Papanastasiou, D., Quaternary evolution of the Corinth rift and its implications for the late Cenozoic evolution of the Aegean. *Geoph. J. Int.*, **126(1)**, pp. 11–53, 1996.

[13] Tselentis, G. & Makropoulos, K., Rates of crustal deformation in the Gulf of Corinth (Central Greece) as determined from seismicity. *Tectonophysics* **124**, pp. 55–66, 1986.

[14] Jibson, R.W., Harp, E.L. & Michael, J.A.A., Method for Producing Digital Probabilistic Seismic Landslide Hazard Maps: An example from the Los Angeles, California, Area. *US Geological Survey Open-File Report 98–113,* 1998.

[15] McCalpin, J.P., An Improved Procedure for Mapping Earthquake-Induced Landslide Potential Using a Geographic Information System, with Application to the Puget Sound Region, Element III.3. *Final technical report, National Earthquake Hazards Reduction Program, US Geological Survey,* 1997.

[16] Jibson, R.W., Predicting earthquake-induced landslide displacements using Newmark's sliding block analysis. *Transportation Research Record,* **1411**, pp. 9–17, 1993.

[17] Dobry, R., Idriss, I.M. & Ng, E., Duration Characteristics of Horizontal Components of Strong-Motion Earthquake Records. *Bulletin of the Seismological Society of America,* **68(5)**, pp. 1487–1520, 1978.

[18] Wilson R.C. & Keefer D.K., Dynamic analysis of a slope failure from the 6 August 1979 Coyote Lake, California, earthquake. *Bulletin of the Seismological Society of America*, 73, pp. 863–877, 1983.

[19] Gruenthal, G. & the GSHAP Region 3 Working Group, Seismic Hazard Assessment for Central, North and Northwest Europe: GSHAP Region 3. *Annali di Geofisica*, GHSAP Special Volume, 1999.